


# Cerebrospinal fluid transcripts may predict shunt surgery responses in normal pressure hydrocephalus

Zachary Levin,<sup>1,2</sup> Owen P. Leary,<sup>3</sup> Victor Mora,<sup>1,2</sup> Shawn Kant,<sup>3</sup> Sarah Brown,<sup>3</sup> Konstantina Svokos,<sup>3</sup> Umer Akbar,<sup>4</sup> Thomas Serre,<sup>2,5</sup> Petra Klinge,<sup>3</sup>  Alexander Fleischmann<sup>1,2</sup> and Maria Grazia Ruocco<sup>2,5</sup>

Molecular biomarkers for neurodegenerative diseases are critical for advancing diagnosis and therapy. Normal pressure hydrocephalus (NPH) is a neurological disorder characterized by progressive neurodegeneration, gait impairment, urinary incontinence and cognitive decline. In contrast to most other neurodegenerative disorders, NPH symptoms can be improved by the placement of a ventricular shunt that drains excess CSF. A major challenge in NPH management is the identification of patients who benefit from shunt surgery. Here, we perform genome-wide RNA sequencing of extracellular vesicles in CSF of 42 NPH patients, and we identify genes and pathways whose expression levels correlate with gait, urinary or cognitive symptom improvement after shunt surgery. We describe a machine learning algorithm trained on these gene expression profiles to predict shunt surgery response with high accuracy. The transcriptomic signatures we identified may have important implications for improving NPH diagnosis and treatment and for understanding disease aetiology.

- 1 Department of Neuroscience, Brown University, Providence, RI 02912, USA
- 2 Carney Institute for Brain Science, Brown University, Providence, RI 02912, USA
- 3 Department of Neurosurgery, Rhode Island Hospital, Warren Alpert Medical School, Brown University, Providence, RI 02903, USA
- 4 Department of Neurology, Rhode Island Hospital, Warren Alpert Medical School, Brown University, Providence, RI 02903, USA
- 5 Department of Cognitive Linguistic and Psychological Sciences, Brown University, Providence, RI 02912, USA

Correspondence to: Maria Grazia Ruocco  
Department of Cognitive Linguistic and Psychological Sciences, 190 Thayer Street, and the Carney Institute for Brain Science  
Brown University, 164 Angel Street,  
Providence, RI 02912, USA  
E-mail: [maria\\_grazia\\_ruocco@brown.edu](mailto:maria_grazia_ruocco@brown.edu)

Correspondence may also be addressed to: Alexander Fleischmann  
Department of Neuroscience and the Carney Institute for Brain Science, Brown University, Providence, RI 02912, USA  
E-mail: [alexander\\_fleischmann@brown.edu](mailto:alexander_fleischmann@brown.edu)

**Keywords:** normal pressure hydrocephalus; CSF transcriptomics; shunt surgery response; machine learning

Introduction

Neurodegenerative diseases represent a large group of neurological disorders caused by the loss of neurons, typically resulting in progressive cognitive, motor and autonomic dysfunction.<sup>1,2</sup> Despite major efforts to address the growing health crisis caused by neurodegenerative diseases, reliable diagnostic tests and effective therapies remain largely unavailable.<sup>3,4</sup>

Normal pressure hydrocephalus (NPH) is a progressive neurological disorder affecting an estimated 20 million people worldwide.<sup>5,7</sup> It is characterized by the accumulation of CSF in the brain ventricles and results in progressive neurodegeneration, locomotor dysfunction, urinary incontinence and cognitive decline.<sup>8,9</sup> NPH has been estimated to account for 5–10% of all dementia cases.<sup>6,7,10</sup> However, because symptoms overlap with those of other neurodegenerative disorders including Alzheimer’s disease (AD) and Parkinson’s disease, accurately differentiating NPH from other neurodegenerative disorders remains challenging.<sup>8,11</sup>

In contrast to other neurodegenerative disorders, NPH patients can be treated by shunt surgery, the placement of a ventriculoperitoneal shunt to drain excess CSF. Shunt surgery can dramatically ameliorate and even reverse patients’ symptoms and prevent progression into dementia.<sup>8,12</sup> However, diagnostic tools to accurately predict responses to shunt surgery are limited. Diagnostic tests have been developed to simulate the response to CSF drainage by utilizing a high-volume CSF tap test or a lumbar CSF drainage. While the positive predictive value of those tests can reach up to 80% in specialized NPH clinics, their negative predictive value has remained critically low.<sup>13–15</sup> Furthermore, shunt surgery is associated with postoperative risks including shunt infection and should be limited to patients who experience symptom improvement.<sup>14,16</sup> Therefore, there is a critical need for an objective, quantitative diagnostic test that can accurately identify patients who most likely benefit from shunt surgery.

Cerebrospinal fluid is an attractive source for the identification of new NPH biomarkers. CSF surrounds the brain and spinal canal and performs vital homeostatic functions including nourishment, waste removal and mechanical protection.<sup>17–19</sup> CSF contains a large variety of metabolites and extracellular signalling molecules, including growth factors, hormones, lipids and RNAs. Importantly, pathological states including neurodegeneration lead to alterations in the molecular composition of CSF.<sup>20,21</sup> Several recent studies suggested that core biomarkers for neurodegeneration and inflammation, such as amyloid- $\beta$  (A $\beta$ ) and tau proteins, IL-6, IL-8 or TNF $\alpha$ , have limited predictive value for shunt surgery outcomes.<sup>22–26</sup>

Therefore, to identify new CSF-based biomarkers for NPH diagnosis and therapy, we collected CSF from 42 NPH patients during placement of a ventriculoperitoneal shunt. We analysed the expression levels of core molecular markers for neurodegeneration, and we performed transcriptomic profiling of extracellular vesicles in CSF. We identified genes and pathways whose expression levels correlate with the presence of urinary and cognitive symptoms before shunt surgery, and with gait, urinary and cognitive symptom improvement after shunt surgery. We then developed a machine learning pipeline to identify candidate genes that are predictive of shunt surgery outcomes. Together, our data provide evidence for the presence of RNA biomarkers in the CSF of NPH patients that may be able to predict shunt surgery benefits with high accuracy.

Table 1 Patient demographics, baseline NPH symptoms and 3-month shunt surgery responses

Patient characteristics	Number (%) Total n = 42
<b>Demographic details</b>	
Median age, years (range)	73 (60–89)
Sex (M:F)	19:23
<b>NPH aetiology</b>	
Idiopathic (iNPH)	39 (92.8%)
Secondary (sNPH)	3 (7.2%)
<b>Diagnostic study results</b>	
Ventriculomegaly on MRI	42 (100%)
<b>Preoperative symptoms: baseline (n = 42)</b>	
Balance/Gait Instability	42 (100%)
Urinary Incontinence	35 (83.3%)
Cognitive Impairment	36 (85.7%)
Modified Rankin Scale score, mean ( $\pm$ SD)	2.50 ( $\pm$ 0.83)
<b>3-Month postoperative symptoms (n = 38)</b>	
All symptoms improved	4/38 (10.5%)
Balance/gait instability improved	22/38 (57.9%)
Urinary incontinence improved	19/31 (61.3%)
Cognitive impairment improved	20/32 (62.5%)
Modified Rankin Scale score, mean ( $\pm$ SD)	2.24 ( $\pm$ 0.88)

Forty-two CSF samples were collected and 38 patients returned 3 months after shunt surgery for follow-up appointments. To calculate the percentage of patients that improved in each symptom category after surgery, the number of patients reporting symptom improvement was divided by the number of patients that initially presented with that symptom. SD = standard deviation.

Materials and methods

Patient cohort recruitment and clinical follow-up

Following recruitment of a pilot cohort of three patients in November 2019, a total of 54 patients with NPH were approached in a CSF disorders specialty neurosurgical clinic at Rhode Island Hospital between 1 Jan 2020 and 1 June 2021 and invited to participate in the study. Six declined to participate and 48 agreed, providing informed consent either directly or with the aid of a legally authorized representative, as per Rhode Island Hospital Institutional Review Board (IRB) authorization (#1492994). CSF samples were collected from 42 patients. In total, 38/42 patients returned for a 3 ( $\pm$ 1) month clinical follow-up postoperatively (Table 1).

Clinical data acquisition

All patients were seen in a NPH specialty clinic by attending neurosurgeons specialized in NPH and other CSF disorders (P.K. and K.S.). To evaluate gait, urinary incontinence and cognitive symptoms before and after shunt surgery, we rated symptoms based on the severity and the level of activity and activities of daily living function as ‘none, mild, moderate and severe’ in each of the three dimensions of gait, incontinence and dementia, as widely proposed and performed by other investigators.<sup>13</sup> A comprehensive clinician reported neurological examination was performed during in person visits, and subjective symptoms and adverse events were documented at each visit. Clinical data were recorded by means of prospective clinician- and patient-reported quality assessment. The symptoms in each of the elements of the NPH symptom triad (gait, urinary incontinence, cognition) were recorded as above and then categorized as ‘improved’ or ‘not improved’.

In terms of gait, patients were considered functionally improved if the quality of at least one of the following ambulation patterns changed: no assistive device or assisted walking; improved from use of walker to use of cane or use of cane to independent walking; obvious change in balance and walking by documented change in stride length; walking speed and foot-to-floor clearance reduction; reduction in the frequency of daily falls. In terms of urinary incontinence, patient report of lower daily frequency or complete resolution of incontinence and urinary urgency episodes was considered improved. In terms of cognition, patients were considered improved if patient and/or family member reported relevant changes in the quality of at least one of the following symptoms: improved forgetfulness; improved thought processing; increase in engaged conversations; resolution of lethargy and depression. Data were entered into the electronic medical record as part of standard clinical documentation and later abstracted by study team members (O.P.L. and S.B.) for use as study endpoints.

### CSF sample processing

Patient CSF samples were collected intraoperatively during ventriculoperitoneal shunt placement procedures. Each 15 ml sample was procured immediately upon placement of the ventricular catheter into a sterile, chilled polypropylene collection tube. The sample was then immediately transferred on ice for processing and storage. Ten millilitres of the sample were centrifuged at 1500 relative centrifugal force (RCF) for 10 min at 4°C to remove debris. Supernatant was collected (~10 ml), flash frozen in liquid nitrogen and stored at –80°C for extracellular vesicle (EV) isolation and mRNA extraction. The remaining 5 ml of the sample was aliquoted into multiple 0.15 and 2 ml polypropylene storage tubes for immunoassay analysis. These samples did not undergo centrifugation and were stored at –80°C.

### ELISA analysis and literature comparison

Forty-one patients were assayed for IL-6, IL-8, TNF $\alpha$  and neurofilament light chain (NFL). Thirty-two patients were assayed for A $\beta$ <sub>42</sub>, p-Tau181 and p-Tau181/total-Tau, due to technical limitations of the ELISA plates. Tests were performed at Quanterix (Billerica, MA, USA), using Single Molecule Array (Simoa) technology.<sup>27,28</sup> All CSF samples were diluted based on internal standards and measured in duplicate. Samples with technical errors precluding quantification were omitted. The mean of replicates for each sample was calculated and represented graphically. The number of samples for each test is specified in the figure legend of [Supplementary Fig. 2](#).

To compare levels of core neurodegeneration markers in this NPH cohort with published data from non-dementia controls and AD patients, we searched for literature reporting levels of neurodegeneration markers in CSF. Concentrations of A $\beta$ <sub>42</sub> in control patients were identified in Sunderland *et al.*,<sup>29</sup> and concentrations of A $\beta$ <sub>42</sub> in AD and NPH patients were identified in Michael MalekAhmadi *et al.*<sup>30</sup> Concentrations of p-Tau231 for control and AD patients were identified in Pilotto *et al.*<sup>31</sup> Concentrations of IL-6 for control and AD patients were identified in Wennström *et al.*<sup>32</sup> Concentrations of IL-8 in control and AD patients were identified in Galimberti *et al.*<sup>33</sup> Concentrations of TNF $\alpha$  for control and AD patients were identified in Hesse *et al.*<sup>34</sup> Concentrations of glial fibrillary acidic protein (GFAP) for control patients (individuals with idiopathic intracranial hypertension) were identified in Michel *et al.*,<sup>35</sup> and concentrations for patients with AD were identified in Benedet *et al.*<sup>36</sup> Concentrations of NFL for control and

AD patients were identified in Dhiman *et al.*<sup>37</sup> Concentrations of IL-8 in NPH patients were identified in Pyykkö *et al.*<sup>38</sup>

### Extracellular vesicle isolation and mRNA extraction

Extracellular vesicle isolation and mRNA extraction were performed at the Extracellular Vesicle Core Facility at Rhode Island Hospital. CSF was centrifuged at 2000g for 20 min at room temperature. The samples were aliquoted and stored at –80°C. The 10 ml frozen CSF aliquots were thawed on ice and diluted 1:1 in PBS. EVs were isolated by ultracentrifugation in UltraClear 30 ml tubes at 100 000 g for 70 min at 4°C. They were resuspended in 100  $\mu$ l of PBS supplemented with 1% DMSO and stored at –80°C. RNA was extracted using the miRNeasy Micro Kit according to the manufacturer's protocol (Qiagen, ID: 217084).

### RNA sequencing and data analysis

cDNA library preparation and paired-end Illumina sequencing on a NovaSeq 6000 sequencing system were performed at The University of Chicago Genomics Facility. Samples were sequenced in two batches. The first set of samples was sequenced with two technical replicates per sample and the second set of samples was sequenced with three technical replicates per sample. FASTQ files were transferred to Brown University's high-performance computing cluster OSCAR using the Globus file transfer system. 'Trim Galore!' (version 0.5.0) was used to remove Illumina adapter sequences from the raw FASTQ files and FastQC (version 0.11.5) was used to assess the quality of the data. Sequencing reads were then aligned to the human transcriptome (Ensembl GrCh38 release 104) using HiSat2 (version 2.1.0) with the –dta flag.<sup>39</sup> Samtools (version 1.9) was used to convert and sort the sam files to bam files in preparation for mapping and alignment. StringTie (version 1.3.4) was used to assemble alignments into transcripts according to the differential expression workflow described in the StringTie manual.<sup>40,41</sup> Each bam file was assembled into transcripts, the assembled transcripts were merged into a non-redundant set of transcripts across all samples, and the bam files were assembled against the merged transcript set to estimate transcript abundances and generate read coverage tables.

### Differential gene expression analysis

The estimated transcript abundances calculated by StringTie were imported into R (version 4.1.2) using the tximport package (version 1.22.0).<sup>42</sup> Transcripts were summarized to the gene level using the tx2gene feature of the tximport function. Principal component analysis (PCA) of the top 1000 genes by mean expression was used to check for batch effects and detect outliers. Since technical replicates clustered together in PCA space, they were combined for all downstream analysis. The number of genes expressed in each sample was 8730.1  $\pm$  2544.2. DESeq2 (version 1.34.0) was used for differential gene expression analysis.<sup>43</sup> All RNA samples were organized into a single DESeqDataSet using the DESeqDataSetFromTximport function. The design formula for each analysis included a sequencing batch variable plus the clinical outcome of interest. Genes that did not have more than 10 counts in at least five samples were filtered out before differential gene expression analysis. Differential gene expression analysis then followed the standard workflow for DESeq2.

## Gene set enrichment analysis

Gene set enrichment analysis was carried out using the GSEA tool (version 4.2.3).<sup>44</sup> Genes were ranked using the Wald statistic calculated by DESeq2 and analysed using the GSEA preRanked function. Kyoto Encyclopedia of Genes and Genomes (KEGG) pathways in the Molecular Signatures Database (MSigDB, version 7.5.1) were used. Pathway enrichment results were visualized and plotted using Python (version 3.10.2) and matplotlib (version 3.5.1). Pathways were considered enriched if they showed a false discovery rate (FDR) < 0.25.

## Feature selection and machine learning

Each 3-month clinical response was treated as an independent, binary classification task: gait improvement, urinary improvement, and cognitive improvement. Technical replicates were combined and samples missing the clinical response were excluded. RNA-sequencing (RNA-seq) counts transformed by the variance stabilizing transformation (vst) function in DESeq2 were exported from R into Python. The Python package scikit-learn (version 1.0.2) was used for all pre-processing and machine learning steps.<sup>45</sup> Leave-One-Out cross validation was used to generate *N* training and testing splits, where *N* was the total number of samples. In each fold, gene expression was z-scored using the StandardScaler function in scikit-learn and genes were selected based on their weight in a logistic regression model. To test how the number of selected genes impacted classifier performance, we varied the number of selected genes between 10 and 1000. For each number of selected genes, a support vector machine (SVM) classifier with *C* = 1 was trained and evaluated. We used these model hyperparameters (SVM, *C* = 1) for all predictions as they showed good performance across the three clinical responses and our sample size prevented us from optimizing hyperparameters through cross-validation. To evaluate the classifier's performance, each sample was held out as a test sample once, and the predictions for all samples were concatenated before calculating the area under the receiver operating characteristic curve (AUC). A SVM trained on the smallest number of genes that produced the highest AUC was used for plotting a receiver operating characteristic (ROC) curve. PCA fit to the expression of the selected genes in the first training set was used to visualize the samples in two dimensions of the feature space.

## Statistical analyses

All statistical analyses were performed using R (version 4.1.2), RStudio (version 2022.02.0-443) and Python (version 3.10.2). Chi-square tests and two-sided Mann–Whitney U-tests with a significance threshold of *P* < 0.05 were used to test for differences in sex and age demographics (Supplementary Fig. 1). For ELISA data in Fig. 2, groups were compared using two-sided Mann–Whitney U-tests with a significance threshold of Benjamini–Hochberg adjusted *P* < 0.05. RNA-seq data in Figs 3 and 4 were analysed in DESeq2 with a significance level of Benjamini–Hochberg adjusted *P* < 0.05. KEGG pathways were tested in GSEA and considered significantly enriched with a FDR < 0.25. Normalized expression of top differentially expressed genes was compared with a two-sided Mann–Whitney U-test with a significance threshold of *P* < 0.05.

## Data availability

Anonymized study data including RNA-seq data are available upon request. The R and Python analysis scripts used for this study are available at the GitLab link [https://gitlab.com/nph\\_biomarkers](https://gitlab.com/nph_biomarkers).

## Results

### Demographics of patient cohort and study design

We collected ventricular CSF samples from 42 NPH patients who underwent shunt surgery at the Center for CSF Disorders of the Brain and Spine at Rhode Island Hospital (Table 1). The median age of the patient cohort was 73 years (range: 60–89; Supplementary Fig. 1) and 19 (45%) of the patients were male. Thirty-nine of the patients were diagnosed with idiopathic NPH (iNPH) and three had secondary NPH (sNPH). Two of the sNPH patients developed NPH following traumatic brain injury. The third sNPH patient was diagnosed with NPH 20 years after resection of a low-grade astrocytoma with subsequent chemoradiation, and after serial imaging demonstrated disproportionate ventricular enlargement without evidence of residual or recurrent tumour over that period. All patients (42/42) showed ventriculomegaly on MRI and reported gait impairment. Thirty-five of 42 patients (83%) reported urinary incontinence, and 36/42 patients (86%) had cognitive impairment (see Supplementary Table 1 for combinations of symptoms). The mean baseline modified Rankin Scale (mRS) score of the cohort was 2.50 (±0.83). In 12 patients, a high-volume (50 ml) lumbar tap test was performed to support the candidacy for shunt placement by an observed improvement in walking speed and stride length post lumbar tap.

Thirty-eight of the 42 patients (90%) reported to the 3-month postoperative follow-up appointment. Four patients (10%) showed improvement in all symptoms, 22 (58%) reported improvement in balance/gait symptoms, 19 (61%) reported improvement in urinary incontinence and 20 patients (62%) reported improvement in cognitive impairment. The mean mRS score at 3-months post shunting was 2.24 (±0.88) (Table 1 and Supplementary Table 1).

Cerebrospinal fluid samples were split into aliquots used for ELISA immunoassay and transcriptome analysis. For transcriptome analysis, EVs were isolated and mRNA extracted before Illumina RNA-seq. RNA-seq data were analysed to identify differentially expressed genes and pathways, and a SVM classifier was used to predict 3-month shunt surgery responses based on pre- and postoperative clinical assessments (Fig. 1).

### Expression of core neurodegeneration markers does not correlate with NPH shunt surgery responses

Many neurodegenerative disorders including NPH are characterized by alterations in the CSF expression levels of Aβ and tau proteins, and increased levels of neuroinflammatory markers including IL-6, IL-8 and TNFα.<sup>23,24,30,46–49</sup> Furthermore, increased expression of markers for neuroaxonal damage (NfL) and glial activation (GFAP) are common features of neurodegenerative disorders.<sup>22,50–53</sup>

We therefore tested whether the CSF expression levels of these core CSF biomarkers for neurodegeneration correlated with gait, urinary or cognitive symptom improvement after shunt surgery in our patient cohort. We found that Aβ<sub>42</sub> and p-Tau181 expression, and the p-Tau181/total-Tau ratio, were similar in patients who showed symptom improvement compared with patients who did not show symptom improvement (two-sided Mann–Whitney U-test with Benjamini–Hochberg correction, all *P* > 0.05; Fig. 2A–C). Similarly, IL-6, IL-8 and TNFα levels were similar across patient groups (two-sided Mann–Whitney U-test with Benjamini–Hochberg correction, all *P* > 0.05; Fig. 2D–F). Finally, NfL and GFAP expression levels were similar across patient groups (two-sided Mann–Whitney U-test with Benjamini–Hochberg correction, all



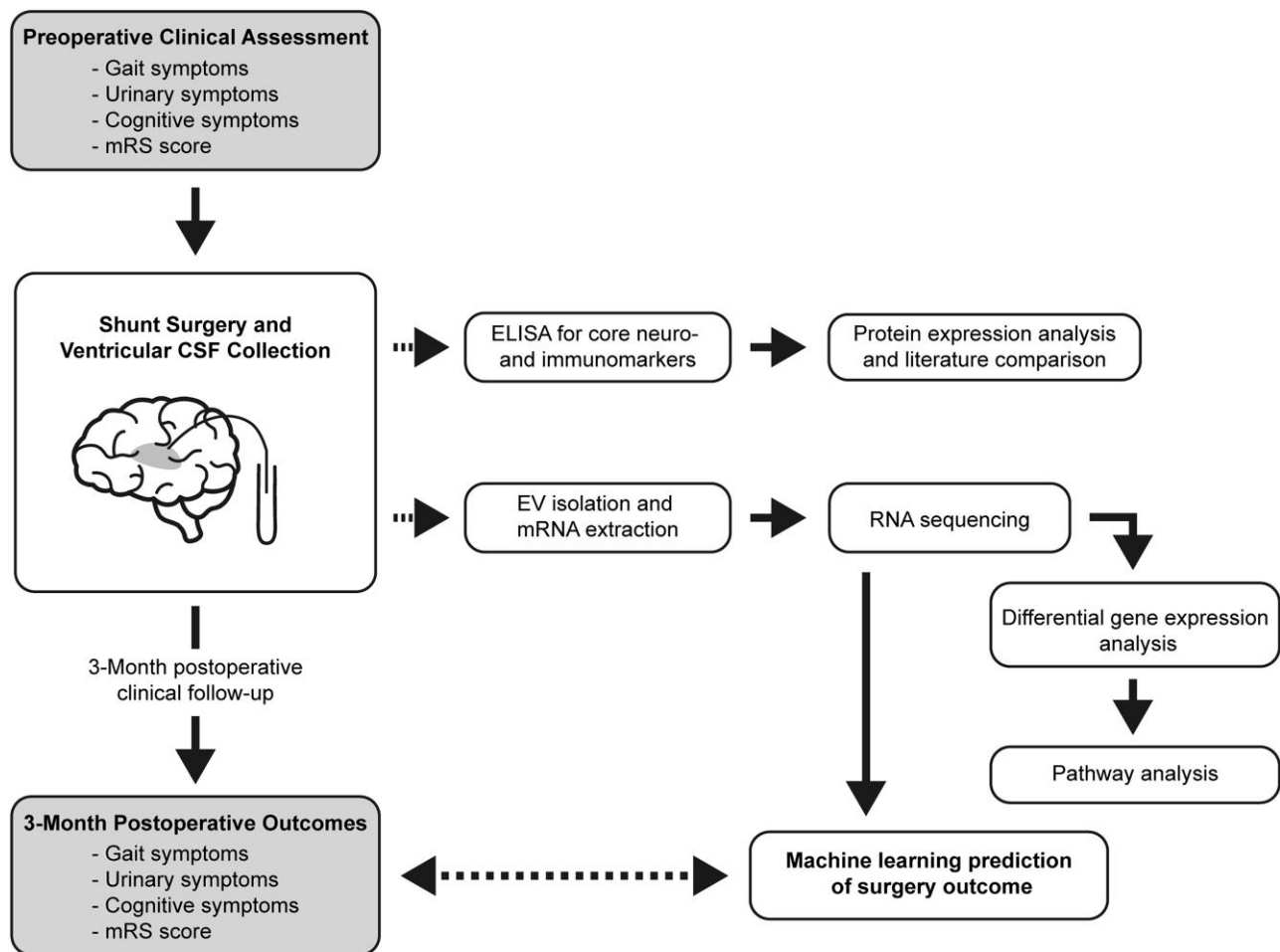


Figure 1 Study design.

$P > 0.05$ ; Fig. 2G and H). Thus, the expression levels of the core neurodegeneration markers  $A\beta_{42}$ ,  $p$ -Tau181, IL-6, IL-8,  $TNF\alpha$ , NfL and GFAP did not correlate with shunt surgery responses in our cohort.

### CSF transcriptome analysis identifies molecular signatures of urinary and cognitive symptoms

NPH patients typically report different combinations of gait, urinary, and cognitive symptoms.<sup>8,9,54</sup> We therefore examined whether the patients' CSF contained transcriptomic signatures that correlated with preoperative NPH symptoms. In this NPH cohort, all patients reported gait impairment. We thus examined whether extracellular vesicles in the CSF contained signatures for urinary incontinence (83% of patients) and cognitive impairment (86% of patients).

Differential gene expression analysis identified 52 genes whose expression was significantly upregulated in patients with urinary incontinence (all Benjamini–Hochberg adjusted  $P < 0.05$ ; Fig. 3A and Supplementary Table 2). To visualize gene expression on a per patient basis, we plotted the normalized expression of the top differentially expressed gene by patient. We found that expression of MOK was significantly increased in patients with urinary symptoms compared to patients without urinary symptoms (two-sided Mann–Whitney U-test,  $P = 0.011$ ; Fig. 3B). By grouping genes into biologically meaningful gene sets, pathway analysis can reduce

noise in transcriptome data and allow for a more robust characterization of molecular changes.<sup>55</sup> We therefore performed pathway analysis using the KEGG pathways, and we identified 12 metabolic pathways that were significantly enriched in patients with urinary incontinence (FDR  $< 0.25$ ; Fig. 3C).

Differential gene expression analysis identified three significantly dysregulated genes in patients with cognitive impairment (all Benjamini–Hochberg adjusted  $P < 0.05$ ; Fig. 3D and Supplementary Table 2). However, on a per patient basis, the expression of *HBG1*, the top differentially expressed gene, was not statistically different between patients with and without cognitive symptoms (two-sided Mann–Whitney U-test,  $P = 0.35$ ; Fig. 3E). Finally, KEGG pathway analysis identified nine metabolic pathways that were significantly dysregulated in patients with cognitive impairment (FDR  $< 0.25$ ; Fig. 3F). Together, these data identify genes and pathways whose CSF expression levels correlate with the presence of urinary and cognitive symptoms in NPH patients.

### CSF transcriptome analysis identifies molecular signatures of NPH shunt surgery responses

We next tested whether CSF gene expression profiles correlated with NPH shunt surgery responses. We performed differential gene expression and pathway analysis for patients who did or did not show symptom improvement 3 months after shunt surgery.

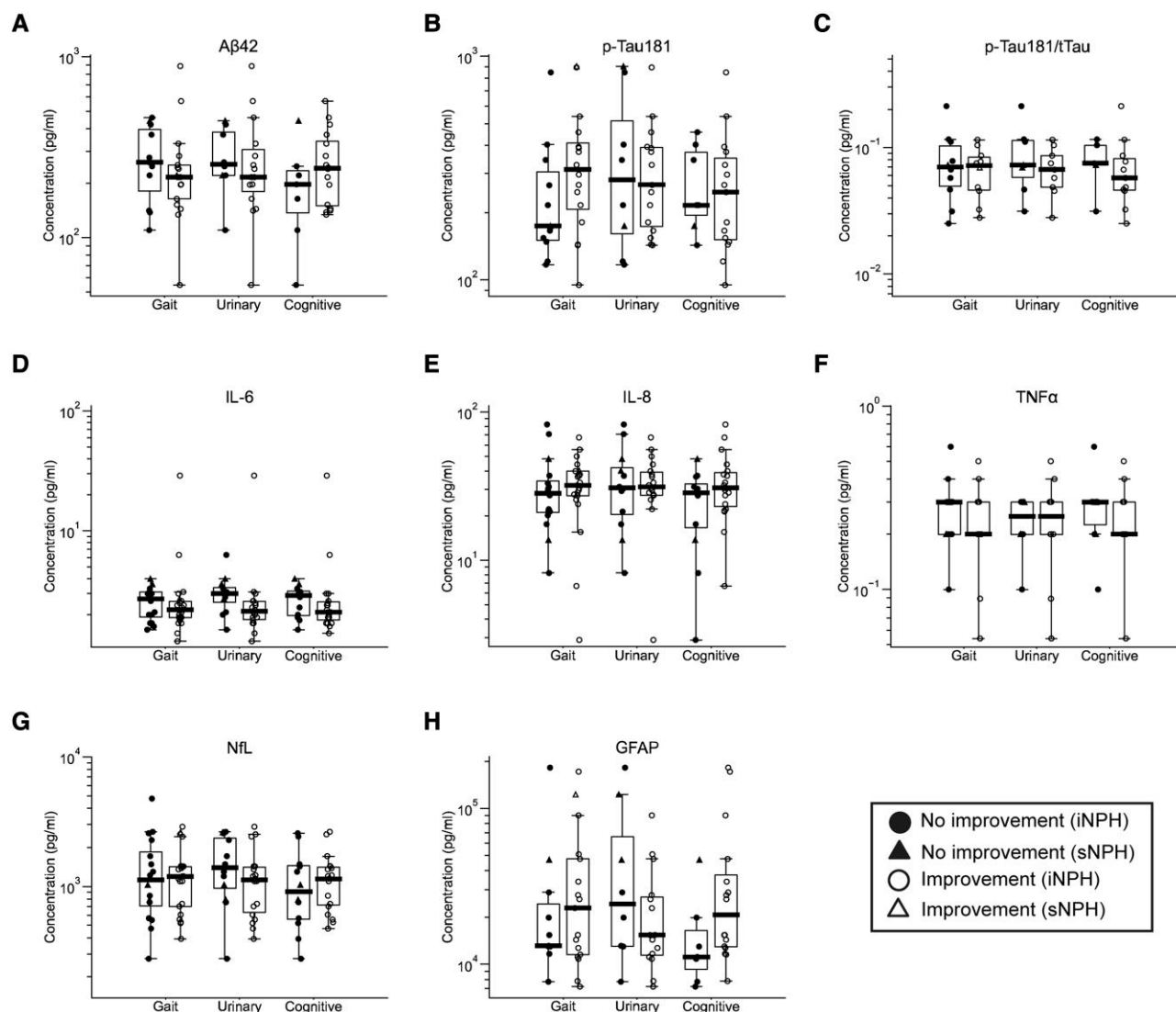


**Figure 2** Concentrations of core CSF biomarkers for neurodegeneration do not correlate with NPH shunt surgery responses. (A) Concentrations of  $A\beta_{42}$  for patients with improvement (open markers) or without improvement (filled markers) in gait, urinary and cognitive symptoms after shunting. Circles indicate iNPH patients and triangles indicate sNPH patients. All *P*-values calculated by two-sided Mann–Whitney *U*-test with Benjamini–Hochberg multiple hypothesis correction (Gait, *U* = 74.5, *P* = 0.35; Urinary, *U* = 48, *P* = 0.37; Cognitive, *U* = 41, *P* = 0.35). (B) Concentrations of p-Tau181 for patients with or without improvement in gait, urinary, and cognitive symptoms after shunting (Gait, *U* = 59.5, *P* = 0.35; Urinary, *U* = 59.5, *P* = 0.5; Cognitive, *U* = 46, *P* = 0.45). (C) Ratio of concentrations of p-Tau181 over total tau (tTau) for patients with or without improvement in gait, urinary and cognitive symptoms after shunting (Gait, *U* = 47, *P* = 0.49; Urinary, *U* = 24, *P* = 0.37; Cognitive, *U* = 21, *P* = 0.37). (D) Concentrations of IL-6 for patients with or without improvement in gait, urinary, and cognitive symptoms after shunting (Gait, *U* = 138, *P* = 0.35; Urinary, *U* = 52.5, *P* = 0.24; Cognitive, *U* = 81.5, *P* = 0.35). (E) Concentrations of IL-8 for patients with or without improvement in gait, urinary, and cognitive symptoms after shunting (Gait, *U* = 137, *P* = 0.35; Urinary, *U* = 105, *P* = 0.49; Cognitive, *U* = 85, *P* = 0.35). (F) Concentrations of TNF $\alpha$  for patients with or without improvement in gait, urinary and cognitive symptoms after shunting (Gait, *U* = 50.5, *P* = 0.35; Urinary, *U* = 48.5, *P* = 0.49; Cognitive, *U* = 42, *P* = 0.35). (G) Concentrations of NfL for patients with or without improvement in gait, urinary and cognitive symptoms after shunting (Gait, *U* = 165, *P* = 0.49; Urinary, *U* = 76, *P* = 0.35; Cognitive, *U* = 100.5, *P* = 0.42). (H) Concentrations of GFAP for patients with or without improvement in gait, urinary and cognitive symptoms after shunting (Gait, *U* = 85, *P* = 0.45; Urinary, *U* = 44, *P* = 0.35; Cognitive, *U* = 26, *P* = 0.29).

We examined three independent, binary outcomes: gait improvement, urinary improvement, and cognitive improvement (Fig. 4). Because iNPH and sNPH represent different neurological conditions, we also performed differential gene expression and pathway analysis for iNPH patients only, omitting the three sNPH patients (Supplementary Fig. 3).

For patients with improvement in gait symptoms, differential gene expression analysis did not identify individual genes that reached statistical significance after multiple hypothesis correction (Benjamini–Hochberg adjusted *P* < 0.05; Fig. 4A). Despite the lack of

statistically significant differentially expressed genes, we plotted the normalized expression of the gene with lowest adjusted *P*-value for each patient to visualize gene expression on a per patient basis. We found that patients with gait improvement had increased expression of *MORN1* (two-sided Mann–Whitney *U*-test, *P* = 0.015; Fig. 4B). Furthermore, KEGG pathway analysis identified 3 pathways that were significantly dysregulated in patients with gait improvement (FDR < 0.25; Fig. 4C).

For patients with improvement in urinary incontinence, differential gene expression analysis did not identify individual genes

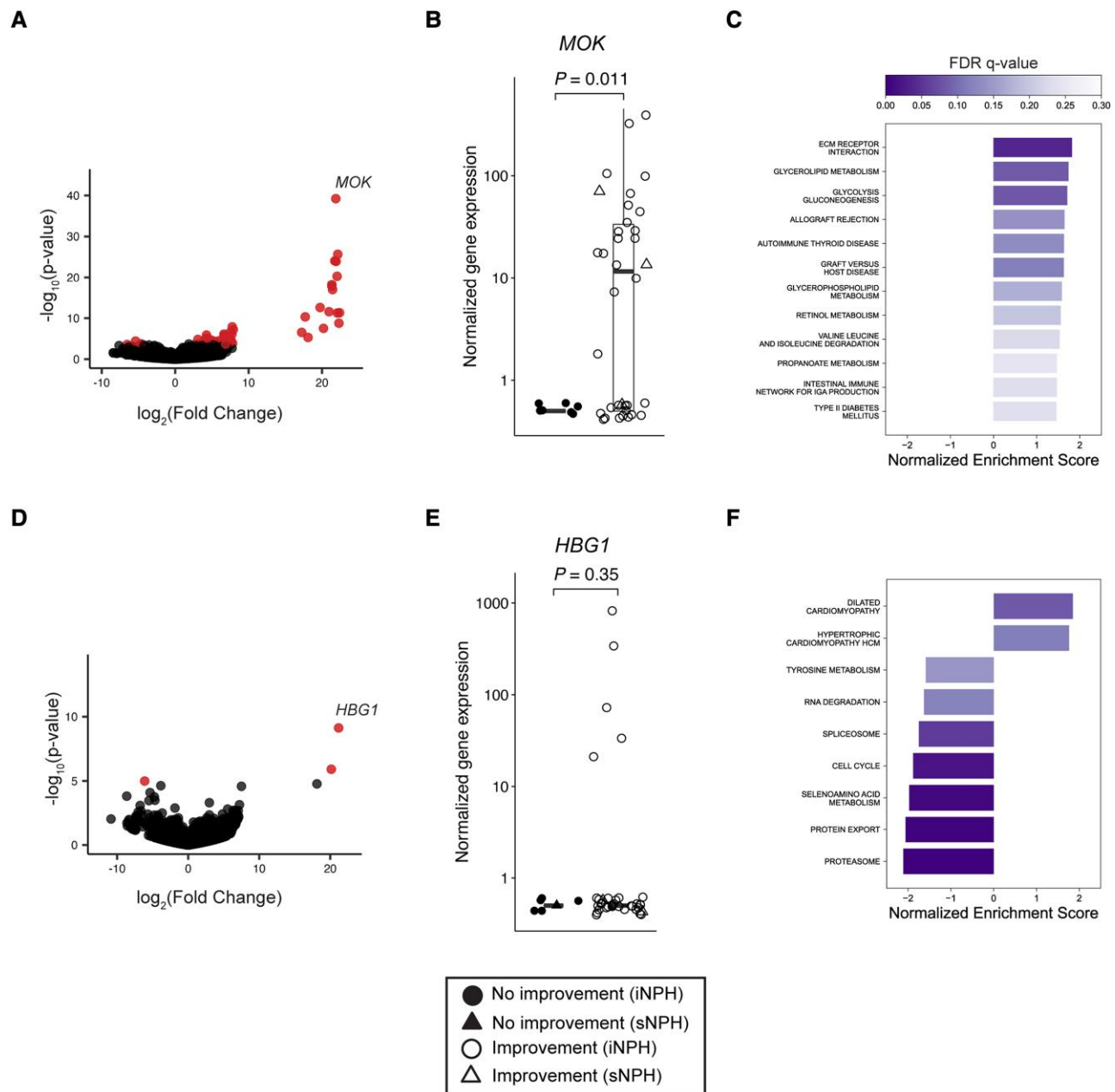


**Figure 3** CSF signatures for urinary incontinence and cognitive impairment in NPH patients. (A) Differentially expressed genes (DEGs) correlated with urinary incontinence. Positive fold change indicates increased expression in patients with urinary incontinence. Red dots indicate genes with Benjamini–Hochberg adjusted  $P$ -value  $< 0.05$ . (B) Normalized expression of *MOK* for each patient. Filled markers = patients without urinary incontinence ( $n = 7$ ); open markers = patients with urinary incontinence ( $n = 35$ ); circles = iNPH patients; triangles = sNPH patients. U- and P-values calculated by two-sided Mann–Whitney U-test ( $U = 52.5$ ,  $P = 0.011$ ). (C) KEGG pathways enriched in patients with urinary incontinence. Positive normalized enrichment scores (NES) indicate upregulation in patients with urinary incontinence. Colour of each bar indicates the FDR q-value. (D) Plot as in A, showing DEGs based on cognitive symptoms in NPH patients. Red dots indicate genes with Benjamini–Hochberg adjusted  $P$ -value  $< 0.05$ . (E) Normalized expression of *HBG1* for each patient. Filled markers = patients without cognitive impairment ( $n = 6$ ); open markers = patients with cognitive impairment ( $n = 36$ ). Circles = iNPH patients; triangles = sNPH patients. U- and P-values calculated by two-sided Mann–Whitney U-test ( $U = 93$ ,  $P = 0.35$ ). (F) KEGG pathways upregulated (positive NES) and downregulated (negative NES) in patients with cognitive symptoms. Colour of each bar indicates the FDR q-value.

that reached statistical significance (Benjamini–Hochberg adjusted  $P < 0.05$ ; Fig. 4D). Nevertheless, expression of *N4BP1* was higher in patients with urinary improvement (two-sided Mann–Whitney U-test,  $P = 0.002$ ; Fig. 4E). KEGG pathway analysis identified two pathways that were significantly dysregulated in patients with urinary improvement (FDR  $< 0.25$ ; Fig. 4F).

Finally, for patients with cognitive improvement after shunt surgery, differential gene expression analysis identified seven

significantly upregulated genes (all Benjamini–Hochberg adjusted  $P < 0.05$ ; Fig. 4G and Supplementary Table 2), and patients with cognitive improvement showed significantly increased expression of *TRIM52-AS1* (two-sided Mann–Whitney U-test,  $P = 0.034$ ; Fig. 4H). KEGG pathway analysis identified five metabolic pathways that were significantly downregulated in patients with cognitive improvement (FDR  $< 0.25$ ; Fig. 4I). Together, these data indicate widespread changes, with broadly varying effect

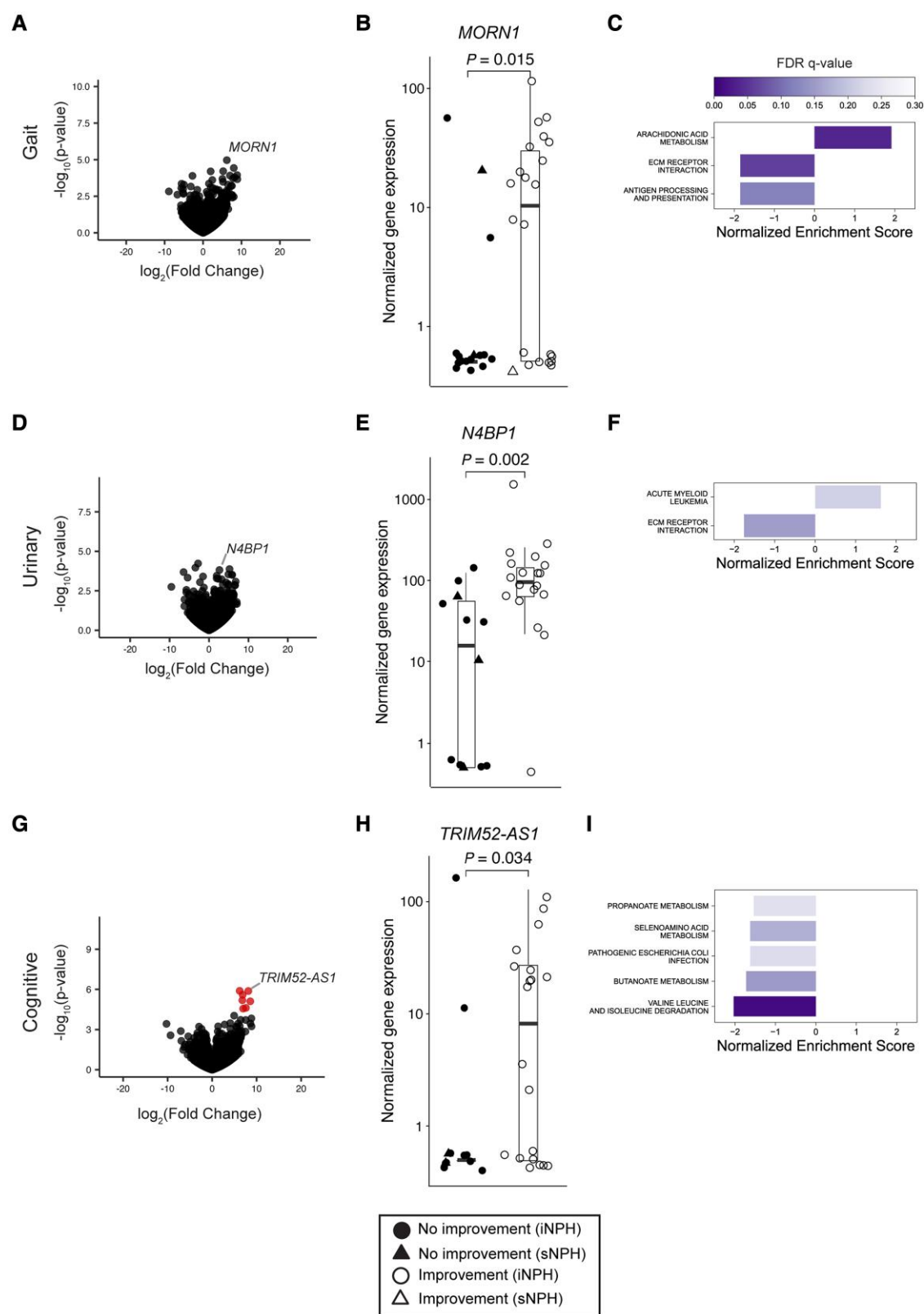


**Figure 4** CSF signatures for gait, urinary and cognitive symptom improvement after shunt surgery. (A) Differentially expressed genes (DEGs) correlated with gait symptom improvement 3 months after shunt surgery. Positive fold-change indicates increased expression in patients with gait improvement. (B) Normalized expression of *MORN1* for each patient. Filled markers = patients without gait improvement ( $n = 16$ ); open markers = patients with gait improvement ( $n = 22$ ). Circles = iNPH patients; triangles = sNPH patients. U- and P-values calculated by two-sided Mann–Whitney U-test ( $U = 101.5$ ,  $P = 0.015$ ). (C) KEGG pathways enriched in patients with gait improvement. Positive normalized enrichment scores (NES) indicate up-regulation in patients with gait improvement. Colour of each bar indicates the FDR q-value. (D) DEGs correlated with urinary symptom improvement

(continued)



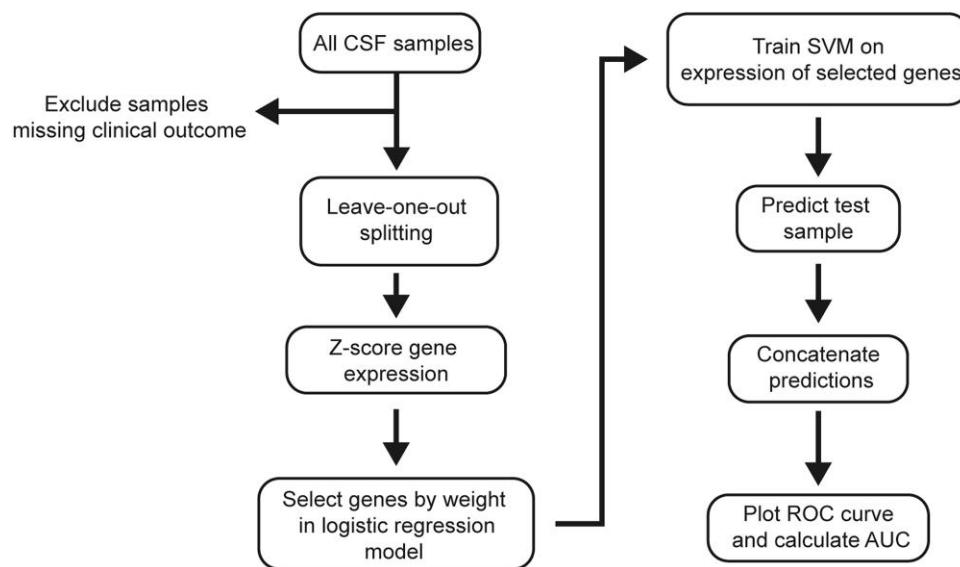


**Figure 5** Feature selection by logistic regression weights and SVM machine learning approach for predicting symptom improvement after shunt surgery

sizes, in the expression of genes and pathways that correlate with improved gait, urinary, and cognitive symptoms after NPH shunt surgery.

### A machine learning classifier to predict shunt surgery responses based on CSF transcriptomes

To test if the changes in CSF gene and pathway expression we identified can predict shunt surgery responses, we developed a machine learning pipeline. Using a leave-one-out cross-validation procedure, we first z-scored gene expression and fitted a logistic regression model to the gene expression data to identify predictive genes as those with the highest weights assigned by the model. Next, we trained a SVM classifier to predict symptom improvement after shunt surgery based on these genes. We then determined the optimal number of genes to predict symptom improvement by varying the number of genes selected in each classifier fold between 10 and 1000. Finally, we calculated the AUC of the SVM classifier trained on the most predictive genes (Fig. 5). The results for the iNPH patients only, omitting the three sNPH patients, are presented in [Supplementary Fig. 4](#) and [Supplementary Table 3](#).

For gait improvement, classifier performance peaked when 30 genes were selected, and a SVM classifier fitted to the expression of the selected genes predicted gait improvement with an AUC = 0.80 (Fig. 6A and B). To visualize class separation, we performed PCA on the genes selected in the first iteration of the classifier, which revealed clear separation of patient groups by clinical

outcome (Fig. 6C). To predict urinary improvement, classifier performance peaked with 140 genes and an AUC = 0.79 (Fig. 6D and E). Plotting the samples along the first two principal components in PCA space revealed clear separation of patient groups by clinical outcome (Fig. 6F). Finally, we found that 50 genes selected from the logistic regression model best predicted cognitive improvement (Fig. 6G). A SVM classifier fitted to the expression of 50 genes predicted cognitive improvement with an AUC = 0.81 (Fig. 6H), consistent with clear separation of patient groups in PCA space (Fig. 6I and [Supplementary Table 3](#)). Together, these results suggest that the CSF of NPH patients in our cohort contains transcriptomic profiles that can distinguish patients based on their response to shunt surgery. Furthermore, a small (~100) set of genes may be sufficient to predict gait, urinary and cognitive symptom improvement.

## Discussion

Neurodegenerative diseases are a major, growing health and economic burden worldwide, and there is an urgent need for improved diagnostic and therapeutic solutions.<sup>56</sup> NPH is unique among dementia-causing disorders because it can be effectively treated by surgical shunt placement.<sup>8,12,13</sup> However, only a fraction of NPH patients who undergo shunt surgery experience symptom improvement, with estimates varying from 30% to 85%.<sup>2,13–16</sup> In the present study, we report that the transcriptomes of EVs extracted from ventricular CSF contain molecular signatures that correlate with the clinical response to shunt surgery outcomes for the

**Figure 4** (Continued)

3 months after shunt surgery. Positive fold-change indicates increased expression in patients with urinary symptom improvement. (E) Normalized expression of N4BP1 for each patient. Filled markers = patients without urinary symptom improvement ( $n = 12$ ); open markers = patients with urinary symptom improvement ( $n = 19$ ). Circles = iNPH patients; triangles = sNPH patients. U- and P-values calculated by two-sided Mann–Whitney U-test ( $U = 37.5$ ,  $P = 0.0020$ ). (F) KEGG pathways enriched in patients with urinary symptom improvement. Colour of each bar indicates FDR q-value. (G) DEGs correlated with cognitive symptom improvement 3 months after shunt surgery. Positive fold-change indicates increased expression in patients with cognitive improvement. Red dots indicate genes with Benjamini–Hochberg adjusted P-value < 0.05. (H) Normalized expression of TRIM52-AS1 for each patient. Filled markers = patients without cognitive improvement ( $n = 12$ ); open markers = patients with cognitive improvement ( $n = 20$ ). Circles = iNPH patients; triangles = sNPH patients. U- and P-values calculated by two-sided Mann–Whitney U-test ( $U = 70$ ,  $P = 0.034$ ). (I) KEGG pathways enriched in patients with cognitive improvement. Colour of each bar indicates the FDR q-value.

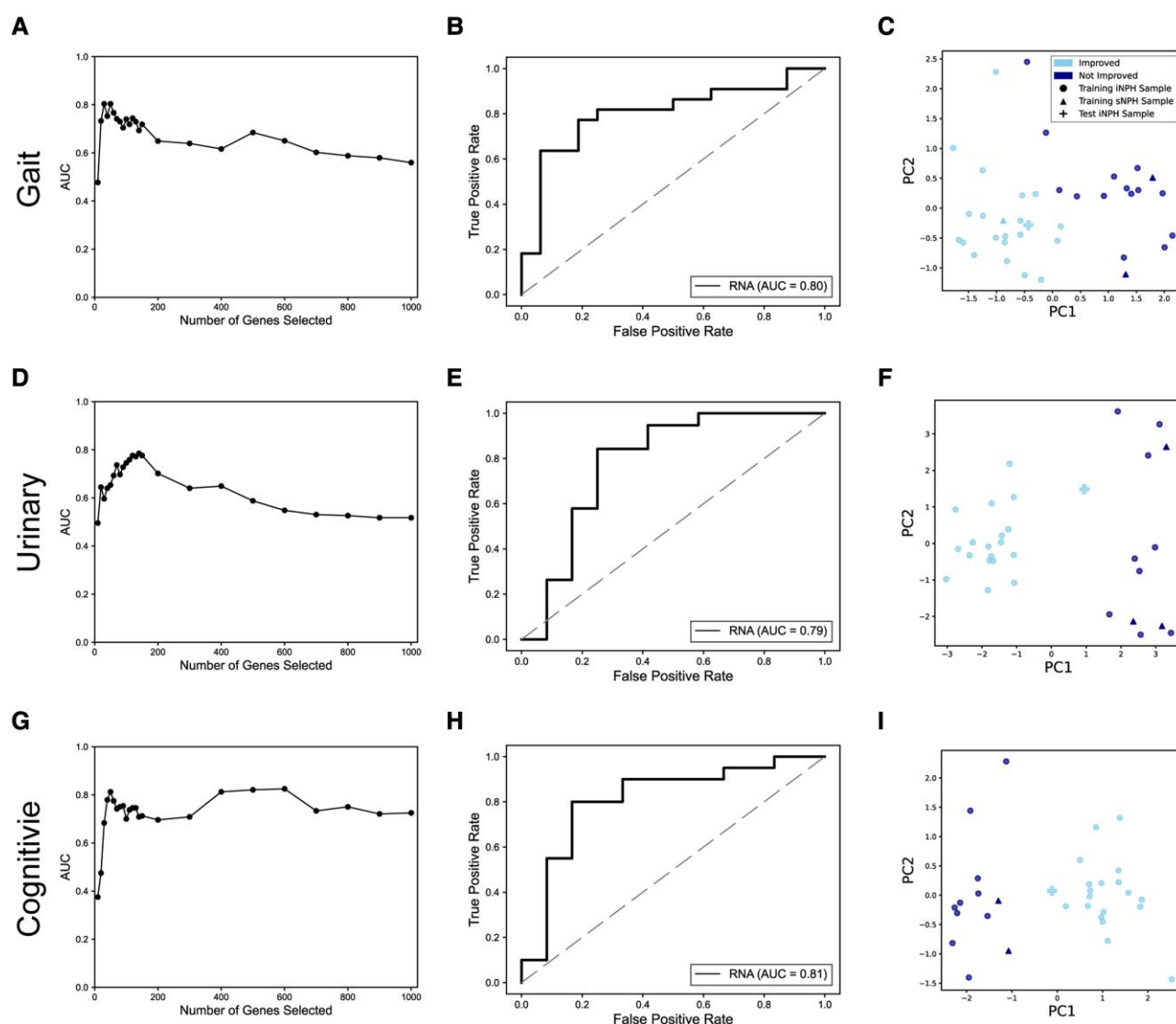


**Figure 6** A machine learning classifier trained on CSF transcriptomic profiles accurately predicts symptom improvement after shunt surgery. (A) Effect of number of genes selected in each classifier fold on predicting gait improvement. (B) ROC curve for predicting gait improvement using 30 genes selected by weights in a logistic regression model. Solid line = prediction based on selected genes; broken line = chance level. (C) PCA plot fit to the training set expression of genes selected when the first sample is the test set. Circles = training set iNPH samples. Triangles = training set sNPH samples; cross = test set iNPH sample; light blue = patients with gait improvement; dark blue = patients without gait improvement. (D) Effect of number of genes selected in each classifier fold on predicting urinary improvement. (E) ROC curve for predicting urinary improvement using 140 genes selected by weights in a logistic regression model. Solid line indicates prediction based on selected genes. (F) PCA plot fit to the training set expression of genes selected when the first sample is the test set. Circles = training set iNPH samples; triangles = training set sNPH samples; cross = test set iNPH sample; light blue = patients with urinary improvement; dark blue = patients without urinary improvement. (G) Effect of number of genes selected in each classifier fold on predicting cognitive improvement. (H) ROC curve for predicting cognitive improvement using 50 genes selected by weights in a logistic regression model. Solid line = prediction based on selected genes. (I) PCA plot fit to the training set expression of genes selected when the first sample is the test set. Circles = training set iNPH samples; triangles = training set sNPH samples; cross = test set iNPH sample; light blue = patients with cognitive improvement; dark blue = patients without cognitive improvement.

classical NPH symptoms (gait/balance impairment, urinary incontinence, and cognitive impairment). Using machine learning, we demonstrate that these molecular signatures can be used to accurately predict shunt surgery responses.

Our cohort of 42 patients, including 39 iNPH and 3 sNPH patients, represents some of the heterogeneity of clinical symptoms typically observed among NPH patients. Through differential gene expression and pathway analysis, we identified genes and pathways whose expression levels correlated with the presence of urinary and cognitive symptoms. These molecular signatures are also candidate biomarkers for the differential diagnosis of

neurodegenerative disorders with clinical symptoms similar to NPH, including AD and Parkinson's disease.<sup>11,23,57</sup>

We also observed widespread changes in gene and pathway expression when comparing shunt surgery responders to non-responders. Based on these observations, we applied a machine learning approach to the CSF transcriptome data to predict shunt surgery responses based on CSF transcriptomic profiling. Our pipeline predicted improvements in gait, urinary, and cognitive symptoms with AUCs of ~0.8, thus substantially improving upon earlier studies relying on common markers for neurodegeneration and inflammation.<sup>22–26</sup>

We envision that our findings could lead to the development of a simple and robust predictive test to improve clinical decision making and NPH patient care. Even without perfect accuracy, a positive CSF-based test result could assist clinicians in the assessment of the potential risks and benefits of shunt surgery, reduce the variability of shunt surgery outcomes reported in the literature, and overall improve patient responses. Furthermore, being able to separately predict which domains of the NPH triad are likely to improve following shunting for a given patient would substantially improve patient care in an individualized manner.

Our machine learning approach allowed us to identify candidate genes and estimate the optimal number of genes required for accurate classification. Our results suggest that a small number of genes may be sufficient for predicting NPH shunt surgery responses. Several of the top predictive genes selected by the classifier have previously been linked to neurodegeneration and play prominent roles in Wnt signalling, oxidative phosphorylation and proteasome function (Supplementary Table 3).<sup>58–60</sup> Together with recently identified genetic risk factors for NPH,<sup>65,66</sup> these genes and pathways provide critical new entry points for the investigation of molecular mechanisms underlying NPH aetiology.

### Limitations of the study

Forty-two NPH patients were included in this study, representing only a fraction of the heterogeneous neurological conditions observed in NPH patients. Future studies with larger patient cohorts will be required to validate the genetic signatures predictive of shunt surgery responses described in this study. Furthermore, studies with larger patient cohorts may reveal distinct molecular signatures for different combinations of symptoms. Finally, studies with larger patient cohorts will be required to determine the extent to which molecular signatures for shunt surgery responses are conserved between iNPH and sNPH patients.

Developing a predictive diagnostic test for the clinic would benefit from the use of CSF obtained through lumbar puncture, rather than CSF collected from the brain ventricles (this study). Lumbar puncture is a minimally invasive procedure that can be performed routinely prior to shunt surgery. Interestingly, while the ventricular system is continuous with the central canal of the spinal cord, differences in the molecular composition of ventricular and lumbar CSF have been reported in the literature.<sup>61–64</sup> Therefore, future studies are needed to comprehensively characterize these differences, and to identify molecular signatures in lumbar CSF that can identify NPH patients who will likely benefit from shunt surgery.

### Acknowledgements

We thank Teah Markstone for help with RNA sequencing analysis, Sicheng Wen and the Lifespan COBRE Center for Stem Cells and Aging for the preparation of extracellular vesicles, and the University of Chicago Genomics Facility for RNA sequencing. We thank Rick Gerkin, Jason Machan and Carsten Eickhoff for advice on statistics and Mark Albers and Justin Fallon for critical comments on the manuscript.

### Funding

This work was supported by a Zimmerman Innovation Award from the Carney Institute for Brain Science and a Brown University OVPR Research Seed Award.

### Competing interests

T. S., P.K. and A.F. are advisors and co-founders of Adelle Diagnostics, Inc. M.G.R. is the CEO and co-founder of Adelle Diagnostics, Inc. The remaining authors report no competing interests.

### Supplementary material

Supplementary material is available at Brain online.

### References

1. Dugger BN, Dickson DW. Pathology of neurodegenerative diseases. *Cold Spring Harb. Perspect. Biol.* 2017;9:a028035.
2. Espay AJ, Da Prat GA, Dwivedi AK, et al. Deconstructing normal pressure hydrocephalus: ventriculomegaly as early sign of neurodegeneration. *Ann Neurol.* 2017;82:503–513.
3. Agrawal M, Biswas A. Molecular diagnostics of neurodegenerative disorders. *Front Mol Biosci.* 2015;2:54.
4. Doroszkiewicz J, Groblewska M, Mroczko B. Molecular biomarkers and their implications for the early diagnosis of selected neurodegenerative diseases. *Int J Mol Sci.* 2022;23:4610.
5. Siraj S. An overview of normal pressure hydrocephalus and its importance: How much do we really know? *J Am Med Dir Assoc.* 2011;12:19–21.
6. Martín-Láez R, Caballero-Arzapalo H, López-Menéndez LÁ, Arango-Lasprilla JC, Vázquez-Barquero A. Epidemiology of idiopathic normal pressure hydrocephalus: a systematic review of the literature. *World Neurosurg.* 2015;84:2002–2009.
7. Andersson J, Rosell M, Kockum K, et al. Prevalence of idiopathic normal pressure hydrocephalus: a prospective, population-based study. *PLoS One.* 2019;14:e0217705.
8. Kiefer M, Unterberg A. The differential diagnosis and treatment of normal-pressure hydrocephalus. *Dtsch. Arzteblatt Int.* 2012; 109:15–25. quiz 26.
9. Tseng P-H, Wu L-K, Wang Y-C, et al. Diagnosis and treatment for normal pressure hydrocephalus: from biomarkers identification to outcome improvement with combination therapy. *Tzu Chi Med. J.* 2022;34:35–43.
10. Jaraj D, Rabiei K, Marlow T, et al. Prevalence of idiopathic normal-pressure hydrocephalus. *Neurology.* 2014;82:1449–1454.
11. Hebb AO, Cusimano MD. Idiopathic normal pressure hydrocephalus: a systematic review of diagnosis and outcome. *Neurosurgery.* 2001;49:1166–1184. discussion 1184–1186.
12. Shprecher D, Schwab J, Kurlan R. Normal pressure hydrocephalus: Diagnosis and treatment. *Curr Neurol Neurosci Rep.* 2008;8: 371–376.
13. Klinge P, Marmarou A, Bergsneider M, Relkin N, Black PM. Outcome of shunting in idiopathic normal-pressure hydrocephalus and the value of outcome assessment in shunted patients. *Neurosurgery.* 2005;57:S40–S52. discussion ii–v.
14. Miyajima M, Kazui H, Mori E, Ishikawa M. on behalf of the SINPHONI-2 Investigators. One-year outcome in patients with idiopathic normal-pressure hydrocephalus: comparison of lumboperitoneal shunt to ventriculoperitoneal shunt. *J Neurosurg.* 2016;125:1483–1492.
15. Vakili S, Moran D, Hung A, et al. Timing of surgical treatment for idiopathic normal pressure hydrocephalus: association between treatment delay and reduced short-term benefit. *Neurosurg Focus.* 2016;41:E2.
16. Feletti A, d'Avella D, Wikkelsø C, et al. Ventriculoperitoneal shunt complications in the European idiopathic normal

- pressure hydrocephalus multicenter study. *Oper. Neurosurg. Hagerstown Md.* 2019;17:97–102.
17. Johanson CE, Duncan JA, Klinge PM, et al. Multiplicity of cerebrospinal fluid functions: new challenges in health and disease. *Cerebrospinal Fluid Res.* 2008;5:10.
  18. Spector R, Keep RF, Robert Snodgrass S, Smith QR, Johanson CE. A balanced view of choroid plexus structure and function: focus on adult humans. *Exp Neurol.* 2015;267:78–86.
  19. Telano LN, Baker S. Physiology, cerebral spinal fluid. *StatPearls.* StatPearls Publishing; 2022.
  20. Tumani H, Teunissen C, Süßmuth S, et al. Cerebrospinal fluid biomarkers of neurodegeneration in chronic neurological diseases. *Expert Rev Mol Diagn.* 2008;8:479–494.
  21. Saugstad JA, Lusardi TA, Van Keuren-Jensen KR, et al. Analysis of extracellular RNA in cerebrospinal fluid. *J Extracell Vesicles.* 2017;6:1317577.
  22. Darrow JA, Lewis A, Gulyani S, et al. CSF Biomarkers predict gait outcomes in idiopathic normal pressure hydrocephalus. *Neurol Clin Pract.* 2022;12:91–101.
  23. Jeppsson A, Wikkelsö C, Blennow K, et al. CSF Biomarkers distinguish idiopathic normal pressure hydrocephalus from its mimics. *J. Neurol Neurosurg Psychiatry.* 2019;90:1117–1123.
  24. Taghdiri F, Gumus M, Algarni M, et al. Association between cerebrospinal fluid biomarkers and age-related brain changes in patients with normal pressure hydrocephalus. *Sci Rep.* 2020;10:9106.
  25. Pfanner T, Henri-Bhargava A, Borchert S. Cerebrospinal fluid biomarkers as predictors of shunt response in idiopathic normal pressure hydrocephalus: a systematic review. *Can J Neurol Sci J Can Sci Neurol.* 2018;45:3–10.
  26. Manniche C, Simonsen AH, Hasselbalch SG, et al. Cerebrospinal fluid biomarkers to differentiate idiopathic normal pressure hydrocephalus from subcortical ischemic vascular disease. *J Alzheimers Dis JAD.* 2020;75:937–947.
  27. Rissin DM, Kan CW, Campbell TG, et al. Single-molecule enzyme-linked immunosorbent assay detects serum proteins at subfemtomolar concentrations. *Nat Biotechnol.* 2010;28:595–599.
  28. Wilson DH, Rissin DM, Kan CW, et al. The simoa HD-1 analyzer: a novel fully automated digital immunoassay Analyzer with single-molecule sensitivity and multiplexing. *J Lab Autom.* 2016;21:533–547.
  29. Sunderland T, Linker G, Mirza N, et al. Decreased beta-amyloid1–42 and increased tau levels in cerebrospinal fluid of patients with Alzheimer disease. *JAMA.* 2003;289:2094–2103.
  30. Michael MalekAhmadi AT. Differences in cerebrospinal fluid biomarkers between clinically diagnosed idiopathic normal pressure hydrocephalus and Alzheimer's disease. *J Alzheimers Dis Park.* 2014;04:1000150.
  31. Pilotto A, Parigi M, Bonzi G, et al. Differences between plasma and CSF p-tau181 and p-tau231 in early Alzheimer's disease. *J Alzheimers Dis.* 2021;87:991–997.
  32. Wennström M, Hall S, Nägga K, et al. Cerebrospinal fluid levels of IL-6 are decreased and correlate with cognitive status in DLB patients. *Alzheimers Res Ther.* 2015;7:63.
  33. Galimberti D, Schoonenboom N, Scheltens P, et al. Intrathecal chemokine synthesis in mild cognitive impairment and Alzheimer disease. *Arch Neurol.* 2006;63:538.
  34. Hesse R, Wahler A, Gummert P, et al. Decreased IL-8 levels in CSF and serum of AD patients and negative correlation of MMSE and IL-1 $\beta$ . *BMC Neurol.* 2016;16:185.
  35. Michel M, Fiebich BL, Kuzior H, et al. Increased GFAP concentrations in the cerebrospinal fluid of patients with unipolar depression. *Transl Psychiatry.* 2021;11:308.
  36. Benedet AL, Milà-Alomà M, Vrillon A, et al. Differences between plasma and cerebrospinal fluid glial fibrillary acidic protein levels across the Alzheimer disease continuum. *JAMA Neurol.* 2021;78:1471.
  37. Dhiman K, Gupta VB, Villemagne VL, et al. Cerebrospinal fluid neurofilament light concentration predicts brain atrophy and cognition in Alzheimer's disease. *Alzheimers Dement Diagn (amst).* 2020;12:e12005.
  38. Pyykkö OT, Lumela M, Rummukainen J, et al. Cerebrospinal fluid biomarker and brain biopsy findings in idiopathic normal pressure hydrocephalus. *PloS One.* 2014;9:e91974.
  39. Kim D, Paggi JM, Park C, Bennett C, Salzberg SL. Graph-based genome alignment and genotyping with HISAT2 and HISAT-genotype. *Nat Biotechnol.* 2019;37:907–915.
  40. Pertea M, Pertea GM, Antonescu CM, et al. Stringtie enables improved reconstruction of a transcriptome from RNA-seq reads. *Nat Biotechnol.* 2015;33:290–295.
  41. Pertea M, Kim D, Pertea GM, Leek JT, Salzberg SL. Transcript-level expression analysis of RNA-seq experiments with HISAT, StringTie and Ballgown. *Nat Protoc.* 2016;11:1650–1667.
  42. Soneson C, Love MI, Robinson MD. Differential analyses for RNA-Seq: Transcript-level estimates improve gene-level inferences. *F1000Res.* 2016;4:1521.
  43. Love MI, Huber W, Anders S. Moderated estimation of fold change and dispersion for RNA-seq data with DESeq2. *Genome Biol.* 2014;15:550.
  44. Subramanian A, Tamayo P, Mootha VK, et al. Gene set enrichment analysis: A knowledge-based approach for interpreting genome-wide expression profiles. *Proc. Natl. Acad. Sci.* 2005;102:15545–15550.
  45. Pedregosa F, Varoquaux G, Gramfort A, et al. Scikit-learn: Machine learning in python. *J Mach Learn Res.* 2011;12:2825–2830.
  46. Blum-Degen D, Müller T, Kuhn W, et al. Interleukin-1 beta and interleukin-6 are elevated in the cerebrospinal fluid of Alzheimer's and de novo Parkinson's disease patients. *Neurosci Lett.* 1995;202:17–20.
  47. Rydbirk R, Elfving B, Andersen MD, et al. Cytokine profiling in the prefrontal cortex of Parkinson's disease and multiple system atrophy patients. *Neurobiol Dis.* 2017;106:269–278.
  48. Chen X, Hu Y, Cao Z, Liu Q, Cheng Y. Cerebrospinal fluid inflammatory cytokine aberrations in Alzheimer's disease, Parkinson's disease and amyotrophic lateral sclerosis: a systematic review and meta-analysis. *Front Immunol.* 2018;9:2122.
  49. Hu WT, Howell JC, Ozturk T, et al. CSF Cytokines in aging, multiple sclerosis, and dementia. *Front Immunol.* 2019;10:480.
  50. Tullberg M, Blennow K, Månsson J-E, et al. Cerebrospinal fluid markers before and after shunting in patients with secondary and idiopathic normal pressure hydrocephalus. *Cerebrospinal Fluid Res.* 2008;5:9.
  51. Ishiki A, Kamada M, Kawamura Y, et al. Glial fibrillar acidic protein in the cerebrospinal fluid of Alzheimer's disease, dementia with Lewy bodies, and frontotemporal lobar degeneration. *J Neurochem.* 2016;136:258–261.
  52. Bartl M, Dakna M, Galasko D, et al. Biomarkers of neurodegeneration and glial activation validated in Alzheimer's disease assessed in longitudinal cerebrospinal fluid samples of Parkinson's disease. *PloS One.* 2021;16:e0257372.
  53. Schulz I, Kruse N, Gera RG, et al. Systematic assessment of 10 biomarker candidates focusing on  $\alpha$ -synuclein-related disorders. *Mov. Disord. Off. J. Mov. Disord. Soc.* 2021;36:2874–2887.



54. Hashimoto M, Ishikawa M, Mori E, Kuwana N. Study of INPH on neurological improvement (SINPHONI). Diagnosis of idiopathic normal pressure hydrocephalus is supported by MRI-based scheme: a prospective cohort study. *Cerebrospinal Fluid Res.* 2010;7:18.
55. Noori A, Mezlini AM, Hyman BT, Serrano-Pozo A, Das S. Systematic review and meta-analysis of human transcriptomics reveals neuroinflammation, deficient energy metabolism, and proteostasis failure across neurodegeneration. *Neurobiol Dis.* 2021;149:105225.
56. Alzheimer's Disease International, Wimo A, Ali G-C, et al. World Alzheimer report 2015—The global impact of dementia: an analysis of prevalence, incidence, cost and trends. <https://www.alzint.org/resource/world-alzheimer-report-2015/>
57. Allali G, Laidet M, Armand S, Assal F. Brain comorbidities in normal pressure hydrocephalus. *Eur J Neurol.* 2018;25:542-548.
58. Purro SA, Galli S, Salinas PC. Dysfunction of Wnt signaling and synaptic disassembly in neurodegenerative diseases. *J. Mol. Cell Biol.* 2014;6:75-80.
59. Singh A, Kukreti R, Saso L, Kukreti S. Oxidative stress: A key modulator in neurodegenerative diseases. *Mol. Basel Switz.* 2019;24:E1583.
60. Schmidt MF, Gan ZY, Komander D, Dewson G. Ubiquitin signaling in neurodegeneration: mechanisms and therapeutic opportunities. *Cell Death Differ.* 2021;28:570-590.
61. Djukic M, Lange P, Erbguth F, Nau R. Spatial and temporal variation of routine parameters: pitfalls in the cerebrospinal fluid analysis in central nervous system infections. *J Neuroinflammation.* 2022;19:174.
62. Konen FF, Lange P, Wurster U, et al. The influence of the ventricular-lumbar gradient on cerebrospinal fluid analysis in serial samples. *Brain Sci.* 2022;12:410.
63. Hirasawa M, de Lange ECM. Revisiting cerebrospinal fluid flow direction and rate in physiologically based pharmacokinetic model. *Pharmaceutics.* 2022;14:1764.
64. Kopkova A, Sana J, Machackova T, et al. Cerebrospinal fluid MicroRNA signatures as diagnostic biomarkers in brain tumors. *Cancers (Basel).* 2019;11:1546.
65. Sato H, Takahashi Y, Kimihira L, et al. A segmental copy number loss of the SFMBT1 gene is a genetic risk for shunt-responsive, idiopathic Normal Pressure Hydrocephalus (iNPH): a case-control study. *PloS One.* 2016;11:e0166615.
66. Yang HW, Takahashi Y, Kimihira L, et al. Deletions in CWH43 cause idiopathic normal pressure hydrocephalus. *EMBO Mol. Med.* 2021;13:e13249.